PHYSICAL REVIEW B **75**, 155322 (2007)

Reversible ferromagnetic switching in ZnO:(Co, Mn) powders

D. Rubi* and J. Fontcuberta
Institut de Ciència de Materials de Barcelona, Campus UAB, E-08193 Bellaterra, Spain

A. Calleja and Ll. Aragonès
Quality Chemicals, Fornal 35, Polígono Industrial Can Comelles Sud, Esparreguera 08292, Spain

X. G. Capdevila and M. Segarra
Facultat de Química, Universitat de Barcelona, Martí i Franquès 1, 08028 Barcelona, Spain
(Received 3 August 2006; revised manuscript received 22 December 2006; published 17 April 2007)

We report here on the magnetic properties of ZnO:Mn- and ZnO:Co-doped nanoparticles. We have found that the ferromagnetism of ZnO:Mn can be switched on and off by consecutive low-temperature annealings in O_2 and N_2, respectively, while the opposite phenomenology was observed for ZnO:Co. These results suggest that different defects (presumably *n*-type for ZnO:Co and *p*-type for ZnO:Mn) are required to induce a ferromagnetic coupling in each case. We will argue that ferromagnetism is likely to be restricted to a very thin, nanometric layer at the grain surface. These findings reveal and give insight into the dramatic relevance of surface effects to the occurrence of ferromagnetism in ZnO-doped oxides.

DOI: 10.1103/PhysRevB.75.155322 PACS number(s): 75.50.Pp, 75.50.Tt, 75.70.Rf

I. INTRODUCTION

The development of diluted magnetic semiconductors (DMSs) with Curie temperatures above room temperature could eventually lead to a generation of spintronic devices with exciting functionalities. Early theoretical claims[1,2] attributed this potential to TM:ZnO (where TM is a transition metal), stimulating intensive studies on the magnetic properties of ZnO doped with different magnetic cations. However, the results obtained up to now have been very controversial. Indeed, the observation of room-temperature ferromagnetism has been attributed either to an intrinsic[3,4] or extrinsic[5,6] property of TM:ZnO, while other reports claim a genuine paramagnetic behavior.[7,8] Furthermore, this controversy is also found even in reports dealing with samples fabricated by similar methods—for example, in nanopowders prepared by means of sol-gel processes.[9,10] This indicates that an intense effort on the understanding of the magnetic interaction of these materials remains to be done.

In agreement with some theoretical predictions,[2] recent experiments suggest that *n*- and *p*-type defects mediate the ferromagnetism of Co:ZnO and Mn:ZnO compounds,[4,11] respectively, raising the possibility of tailoring the ferromagnetic interaction of these materials by modifying their defects structure. For instance, it has been shown that the ferromagnetism of both epitaxial[4,12] and nanoparticle thin films[13,4] of Co:ZnO can be reinforced by exposing them to Zn vapor, which was recently shown to generate zinc interstitials (Zn_i) *n*-type defects.[14] On the other hand, fast annealings of Mn:ZnO nanocrystals capped with N-rich molecules[4] have been shown to enhance their ferromagnetism. It has been claimed that this effect results from the introduction of *p*-type N_O defects. The aforementioned correlation between ferromagnetism and point defects supports the bound magnetic polaron (BMP) model for ferromagnetism in diluted magnetic semiconductors.[15] According to this model, the magnetic exchange among magnetic impurities is mediated by carriers in a split-spin impurity band derived from extended donor orbitals. The opposite polarity of the carriers necessary to mediate the ferromagnetic coupling in Co:ZnO and Mn:ZnO has been related to the different positions of the magnetic impurities and point-defect energy levels in the ZnO band gap, which allows an efficient magnetic impurity-defect hybridization only in the cases of *n*-type Co:ZnO and *p*-type Mn:ZnO.[11]

Being settled the key role played by point defects on the stabilization of the ferromagnetism of ZnO-based diluted magnetic semiconductors, it is evident that the achievement of intrinsic ferromagnetism in these materials is strongly linked to the ability to control their point-defects structure. Here, we will show that the ferromagnetism of Co:ZnO and Mn:ZnO nanopowders can be successively switched on and off by low-temperature annealings under suitable atmospheres. The obtained results demonstrate both the correlation between defects and ferromagnetism *and* the distinct polar behavior of Co:ZnO and Mn:ZnO. We will argue that the modification of the electronic structure of the ZnO surface, either by point defects or by gas chemisorption, controls the sample magnetization.

II. EXPERIMENT

Several series of nanopowders, with nominal stochiometries $Co_{0.1}Zn_{0.9}O$ and $Mn_{0.1}Zn_{0.9}O$, were prepared by means of the acrilamide polymerization method (see Ref. 16 for a detailed description of the preparation method). The obtained xerogels after self-combustion (labeled ZC1 and ZM1 for Co and Mn:ZnO, respectively) were grinded and fired in air for 12 h in a muffle furnace at temperatures T_S of 300, 400, 500, and 600 °C. Here, we will present representative results corresponding to the series labeled as ZC1_T_S and ZM1_T_S, where T_S is the final firing temperature. We have performed thermogravimetric (TGA) experiments on ZC1 and ZM1 samples finding no substantial weight variations up to

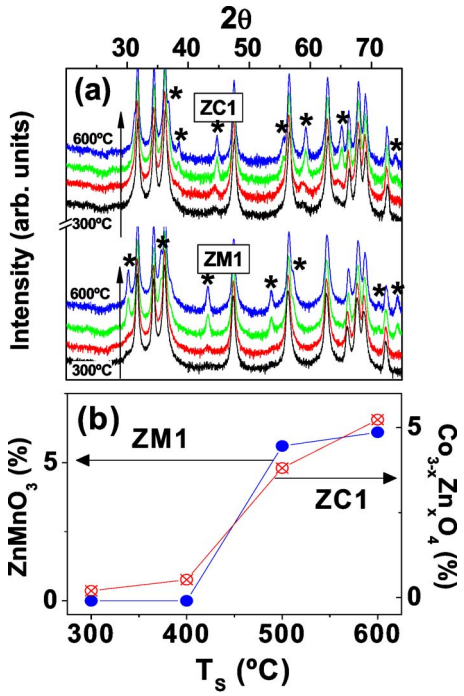

FIG. 1. (Color online) (a) High-resolution XRD patterns corresponding to ZC1 (upper) and ZM1 (lower) series, fired for 12 h in air at temperatures (T_S) of 300, 400, 500, and 600 °C (the arrows signal the raise of T_S). The intensities are shown in logarithmic scale. The peaks indicated with (*) reflect the segregation of impurities [$(ZnCo)_3O_4$ and $ZnMnO_3$ for ZC1 and ZM1 series, respectively]. (b) Concentration of the segregated $(ZnCo)_3O_4$ and $ZnMnO_3$ phases as a function of the firing temperature T_S. $(ZnCo)_3O_4$ concentrations (defined as the ratio between impurity and total masses) were extracted from the corresponding Rietveld refinements, while the amounts of $ZnMnO_3$ were evaluated from the ratio between the 30.2° peak of $ZnMnO_3$ and the 31.7° peak of ZnO.

600 °C, signaling that a complete decomposition of the organic precursos takes place during self-combustion. Structural characterization was performed by x-ray diffraction (Siemens D-5000, using Cu $K_{\alpha 1,\alpha 2}$ radiation) and field emission gun high-resolution transmission electronic microscopy (FEG-TEM) (Jeol 2019F). The particle size was estimated from the broadening of selected x-ray diffraction (XRD) peaks, obtaining crystallite sizes of ~40 nm. The cationic composition was checked by energy dispersive x-ray spectroscopy (EDS), finding in all cases Mn/Zn and Co/Zn ratios consistent with the nominal stoichiometry. Magnetic measurements were performed by means of a superconducting quantum interference device from Quantum Design.

III. RESULTS AND DISCUSSION

Figure 1(a) shows the XRD patterns corresponding to ZM1 and ZC1 samples fired at T_S between 300 and 600 °C. The spectra are dominated by reflections corresponding to the hexagonal wurtzite structure of ZnO [space group (SG) $P6_3mc$]; however, the XRD patterns reveal that increasing the calcination temperature (T_S) favors the emergence of additional peaks (marked with *) that reflect the segregation of the oxide $ZnMnO_3$ and the cubic spinel $Zn_xCo_{3-x}O_4$ (SG $Fd3m$), respectively. No additional reflections associated with other segregated phases were detected. The amount of segregated $Zn_xCo_{3-x}O_4$ was evaluated from the Rietveld refinements of the corresponding XRD patterns. In the case of $ZnMnO_3$, Rietveld refinements are not possible since its structure remains undetermined.[17] In consequence, the concentration of $ZnMnO_3$ as a function of T_S has been simply estimated from the ratio between the ~30.2° peak of $ZnMnO_3$ and the ~31.7° peak of ZnO. Figure 1(b) clearly shows the progressive segregation of $Zn_xCo_{3-x}O_4$ and $ZnMnO_3$ when increasing T_S. The cell volume of the wurtzite phase of the ZM1 series was found to shrink from 48.11(1) Å^3 (ZM1_300 sample) to 47.80(1) Å^3 (ZM1_600 sample) when increasing T_S. Bearing in mind the Mn^{2+} and Zn^{2+} ionic radii (0.66 and 0.60 Å, respectively), the cell contraction reflects the migration of the larger Mn cations out from the wurtzite structure to form the $ZnMnO_3$ impurity. In the case of Co-doped samples, we have found that the cell volume remains in all cases close to the bulk ZnO value (47.62 Å^3). This is related to the similar ionic radii of Co^{2+} and Zn^{2+} (0.58 and 0.60 Å, respectively), which leads into a wurtzite unit cell rather insensitive to Co contents. Detailed high-resolution TEM analysis[18] failed to detect other segregated phases than those observed by XRD. In particular, we should remark that the existence of segregated metallic Co or Mn was not appreciated in any case. Optical absorption and x-ray photoemission spectroscopy experiments, performed on ZM1_300 and ZC1_300 samples, suggest a 2+ valence state and tetrahedral coordination for both Co and Mn ions, indicating that they replace Zn ions in the wurtzite structure.

Figures 2(a) and 2(b) show the evolution of the room-temperature magnetization as a function of the applied field for both ZM1 and ZC1 series. The magnetic moments per atom were evaluated by considering the nominal concentration of magnetic ions. It is found that Mn:ZnO and Co:ZnO samples fired at 300 °C display a clear ferromagnetic response superimposed to a paramagnetic component. In contrast, samples treated at higher temperatures are paramagnetic-like. The saturation magnetizations of ZM1_300 and ZC1_300 samples are rather small (~$0.01\mu_B$/Co and ~$0.002\mu_B$/Mn, respectively). This observation, which is in agreement with many reported data for both bulk samples[19,20] and thin films,[13,21] indicates that only a small fraction of the available magnetic ions are ferromagnetically coupled. The insets in Figs. 2(a) and 2(b) show the temperature dependence of the inverse magnetic susceptibility (χ^{-1}) for ZM1_500 and ZC1_500 samples; in agreement with the magnetization loops, data do not display any ferromagnetic signature. Following Ref. 7, the observed $\chi^{-1}(T)$ dependence can be well fitted by assuming that the susceptibility contains two contributions: (i) a Curie-Weiss term $\chi = C_1/T - \theta_p$, ($\theta_p < 0$) and (ii) a Curie term ($\chi_2 = C_2/T$). The first terms takes into account the antiferromagnetic exchange between near-neighbor magnetic ions (TM–O–TM bonds), while the second one describes the behavior of isolated magnetic atoms. Solid lines through the data points in the insets of Figs. 2(a) and 2(b) are the results of the fits; it can be

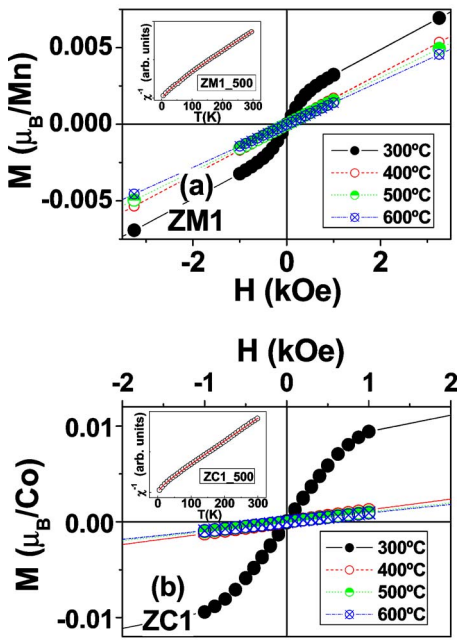

FIG. 2. (Color online) Room-temperature hysteresis loops corresponding to (a) ZM1 and (b) ZC1 samples fired at temperatures between 300 and 600 °C. The diamagnetic contribution of the sample holder was carefully discounted in all cases. The insets show the evolution of the magnetization as a function of the temperature for ZM1_500 and ZC1_500 samples (open symbols) and the corresponding fittings (solid lines, see the text for details).

appreciated that the model accurately reproduces the experimental data. For paramagnetic samples of the ZM1 series, the extrapolated temperatures θ were in the range of $\sim -120/-190$ K, while for the ZC1 series the corresponding values were in the range of $\sim -25/-50$ K. The relative fractions of paramagnetic ions $C_2/(C_1+C_2)$ were found to be $\sim 40\%-50\%$ and $\sim 25\%-35\%$ for ZM1 and ZC1 series, respectively. The obtained θ values for Co-doped samples are larger than those obtained for Mn-doped samples, indicating a stronger antiferromagnetic coupling in the case of Mn–O–Mn bonds.

At this point, it is necessary to discuss about the origin of the ferromagnetic behavior observed in the samples processed at low temperature (300 °C), paying special attention to the possible presence of extrinsic mechanisms. We first notice that the observed impurities ($Zn_xCo_{3-x}O_4$ and $ZnMnO_3$) cannot account for a room-temperature ferromagnetic behavior: the cubic spinel $Zn_xCo_{3-x}O_4$ is ferrimagnetic at low temperatures ($T_C < 50$ K),[22] while $ZnMnO_3$ has been described as a spin glass with a blocking temperature of ~ 15 K.[23] Moreover, Figs. 1(b) and 2 clearly show that the fraction of segregated secondary phases and the sample magnetization follow opposite trends when T_S is increased, thus strongly denying the observed secondary phases as responsible for the measured ferromagnetism. We recall that the usual origin of extrinsic ferromagnetism in Co:ZnO is metallic Co precipitates,[5] which have not been observed in our samples neither by XRD or high-resolution TEM. Similarly, extrinsic ferromagnetism in Mn:ZnO has been proposed to arise from a metastable $(ZnMn)_2O_3$ phase[6] or from interface effects between Zn-rich Mn_2O_3 and MnO_2 interfaces;[24] none of these mechanisms appear to be dominant in our samples as we have failed to detect the presence of Mn_2O_3 or MnO_2 impurities. Therefore, we conclude that the observed ferromagnetism in our ZM1_300 and ZC1_300 samples is a genuine property of these oxides. This conclusion is also supported by the observation (see below) of reversible switching of ferromagnetism in these samples.

Interestingly enough, we have found that the ferromagnetism of as-grown of ZM1_300 and ZC1_300 samples—which have been stored at room temperature for a period of ~ 2 months—vanishes with time, leading to a fully paramagnetic response.[25] We have not been able to observe any significant change in the high-field slope of the hysteresis loops of ZM1_300 and ZC1_300 samples upon aging, indicating that the relative variation of the number of paramagnetic ions is rather small and any modification in their magnetic response remains below the experimental error. The magnetic aging was not accompanied by any detectable structural or chemical modification, suggesting that it may be related to variations of the defect structure of the samples. The time scale of the observed aging is consistent with reported photoluminescence (PL) experiments on pure ZnO samples, where it was shown that a spontaneous and continuous quenching of the PL green band (~ 2.5 eV)—usually ascribed to the presence of point defects[26]—takes place even one year after the sample fabrication.[27] On the other hand, it has been observed that the green PL band of pure ZnO can be modified in a faster and a more controlled way by annealing under different atmospheres such as O_2 or N_2.[27,28] We have, therefore, annealed the "magnetically aged" ZM1_300 and ZC1_300 samples at 300 °C under different atmospheres: air, O_2, N_2, or H_2-Ar (5%). Interestingly enough, we have found that the ferromagnetism of ZC1_300 sample can be regenerated *only* under N_2 atmosphere, as can be observed in Fig. 3(a), while the ferromagnetism of ZM1_300 sample can be switched on *only* under O_2 annealing [Fig. 3(b)]. Figure 3(a) shows that the ferromagnetic component of the ZC1_300 sample monotonically increases with the N_2 time annealing. After a 40 h treatment, the saturation magnetization is raised from ~ 0 to $\sim 0.0018\mu_B$/Co. In the case of ZM1_300 sample, the enhancement of the ferromagnetism is not monotonic with the O_2 time annealing, displaying a maximum saturation magnetization $\sim 0.0026\mu_B$/Mn for a 12 h treatment. Annealed samples were carefully analyzed by XRD and HRTEM, finding in all cases that their structural and chemical properties remain unmodified. This supports the idea that only the defects structure of the samples is varied upon annealing. The regenerated ferromagnetism can be quenched again by performing further treatments under the "opposite" atmospheres: N_2 for Mn:ZnO and O_2 for Co:ZnO. This is illustrated in Fig. 4(a), where it can be seen that successive 300 °C treatments under O_2 (12 h) and N_2 (20 h) atmospheres can switch on and off the ferromagnetism of Mn:ZnO, while the inverse phenomenology is found for Co:ZnO [Fig. 4(b)].

The observed "polar" behavior of Mn:ZnO and Co:ZnO [see Fig. 4(c)] strongly reminds us of the suggested link between the occurrence of ferromagnetism in Co:ZnO and Mn:ZnO with the existence of *n*- and *p*-type defects,

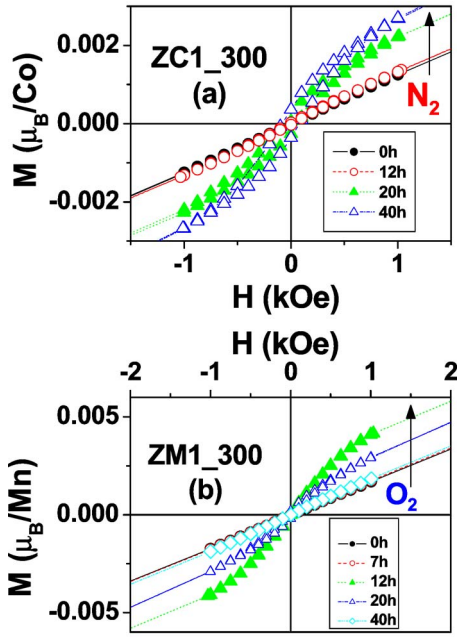

FIG. 3. (Color online) (a) Room-temperature magnetization as a function of the applied field corresponding to the aged ZC1_300 sample, annealed in N_2 at 300 °C for different times (between 12 and 40 h). (b) Room-temperature magnetization as a function of the applied field of the aged ZM1_300 sample, annealed in O_2 at 300 °C for different times (between 7 and 40 h).

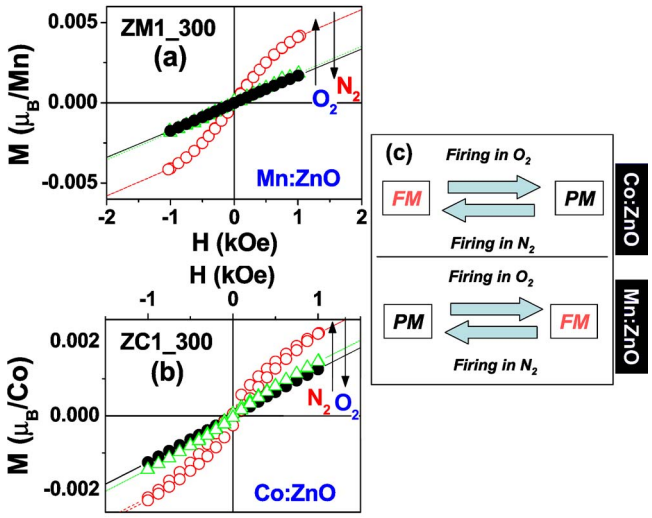

FIG. 4. (Color online) Room-temperature hysteresis loops corresponding to (a) ZM1_300 sample after successive annealings in O_2 (12 h, 300 °C) and N_2 (20 h, 300 °C) and (b) ZC1_300 sample after successive annealings in N_2 (20 h, 300 °C) and O_2 (20 h, 300 °C). It is found that the ferromagnetism in Mn:ZnO can be switched on and off by consecutive annealings in O_2 and N_2, respectively. The opposite behavior is found for Co:ZnO. The scheme in (c) summarizes the observed phenomenology.

respectively.[4,11] Within this framework, it can be inferred that the *n*- and *p*-type characters of our samples are improved by N_2 and O_2 annealing, respectively. In the first case, it can be argued that the inert character of the N_2 atmosphere may lead to the generation of donor oxygen vacancies (V_O). It follows that an analogous effect would be expected after similar annealing under other inert or reducing atmospheres such as Ar or H_2-Ar (5%). However, we have not been able to induce ferromagnetism with other gases than N_2, thus suggesting that N_2 should play an active role on the formation of *n*-type defects such as, for example, the double donor $(N_2)_O$.[29] In the case of O_2 annealing, the most plausible effect is the cancellation of native oxygen vacancies, which may reduce the *n*-type character of the material and eventually allow some previously compensated native acceptors to hybridize with Mn ions and mediate the ferromagnetic coupling.

Finally, we would like to address the key—but puzzling—observation of substantially reduced magnetization values with respect to the expected transition metals moments. We recall that the observed values were $\sim 0.01\mu_B$/Co and $\sim 0.002\mu_B$/Mn for the as-grown ZC1_300 and ZM1_300 samples, while the expected values for Co^{2+} and Mn^{2+} high-spin ions are $3\mu_B$/Co and $5\mu_B$/Mn, respectively. We stress that rather marginal magnetization values have been frequently observed in reports dealing with polycrystalline samples.[9,19,20,30,31] We first notice that a substantial magnetization reduction should indeed be expected due to the presence of antiferromagnetic coupled metal ions. In the case of the ZC1_300 sample, for instance, if we assume as an upper-bound limit that Co spins displaying antiferromagnetic interactions [$\sim$75% of the total, as determined from the fittings of the $\chi^{-1}(T)$ data] do not contribute to the ferromagnetic signal, the estimated magnetization for this sample would be of about $0.04\mu_B$/Co; obviously, this value is still considerably smaller than the expected one, suggesting that only a small fraction of the available Co ions interact ferromagnetically. The annealing process is performed at low temperature and thus the diffusivity of defects should be necessarily small. In the simplest picture, if we assume spherical ZnO particles with radius $R \sim 20$ nm and an overall magnetization $M_S \sim 0.04\mu_B$/Co, a fully saturated ($M_S = 3\mu_B$/Co) thin ferromagnetic layer of about one ZnO unit cell is enough to account for the observed magnetization. For instance, if we use as an upper bound a diffusion coefficient of O_2 of about $\sim 5 \times 10^{-17}$ cm^2/s (as determined at 900 °C for pure ZnO polycrystals[32]), it is found that a processing time of 12 h would give a profile with a characteristic depth ($1/e$ decay) of about 10 nm. This rough estimate suggests that the defect structure modification upon 300 °C annealing can only take place in a very thin surface layer of ZnO ($\ll 10$ nm), and it is just this layer which originates the ferromagnetism. We should note that the latter discussion has assumed that the defects created by annealing are point defects located near the surface; however, we should stress that the existence of purely surface defects—arguably related to the chemisorption of O_2 or N_2 gas upon low-temperature annealing—could also account for similar effects.[33] For instance, it was shown that holes can be induced in ZnO by O_2 chemisorption at low temperatures,[33] which may explain the generation of ferromagnetism in our Mn:ZnO samples upon O_2 annealing.

In any case, the proposed scenario suggests that the defects necessary to stabilize the ferromagnetism are surface related, and thus it is clear that the specific surface of the samples should critically determine their magnetization. This

is likely the reason for the common observation of reduced magnetization in bulk materials; on the contrary, nanometric particles may display larger magnetization. Indeed, a large magnetization of $\sim 1.5\mu_B$/Mn was reported—up to the authors best knowledge—only for ~5 nm Mn:ZnO nanoparticles.[4] Before concluding, we would like to mention that our analysis has implicitly assumed that the observed ferromagnetism arises from the interaction among magnetic moments of magnetic impurities (Co and Mn in our case), as suggested in Refs. 1 and 15. Indeed, we have explored the properties of undoped (Co or Mn free) ZnO particles prepared and processed under the same conditions and treated under O_2 or N_2 atmospheres, finding in all cases a diamagnetic behavior without any signature of ferromagnetism. In consequence, the substitution of Zn atoms by transition metal ions appears to be linked to the appearance of ferromagnetism. However, this scenario neglects the possible contribution to the ferromagnetic response of the orbital magnetic moments associated with the perturbation of electronic clouds at the grain surface, a mechanism that was reported to originate weak ferromagnetism in capped-Au nanoparticles[34] and, very recently, in capped ZnO nanoparticles.[35] New experiments should be designed in order to elucidate which of these mechanisms are indeed associated with the appearance of ferromagnetism in these interesting diluted magnetic semiconductors systems.

IV. CONCLUSIONS

In summary, we have shown that both defects and their donor or acceptor character play a major role in the stabilization of ferromagnetism of TM:ZnO oxides. We have proposed that relevant defects—either point defects or electronic defects associated with gas chemisorption—are likely restricted to a thin nanometric shell covering the particles core, signaling thus a focus for further research on ferromagnetism in ZnO.

ACKNOWLEDGMENTS

We acknowledge financial support from project MAT2005-5656-C04-01. Quality Chemicals would like to thank CIDEM-Generalitat de Catalunya (Contract No. RDITCRIND04-0153) for financial support. Enlightening discussions with A. Hernando are gratefully acknowledged.

*Present address: Zernike Institute for Advanced Materials, University of Groningen, Groningen 9747AG, The Netherlands. Electronic address: d.rubi@rug.nl

[1] T. Dietl, H. Ohno, F. Matsukura, J. Cibert, and D. Ferrand, Science **287**, 1019 (2000).
[2] K. Sato and H. Katayama-Yoshida, Jpn. J. Appl. Phys., Part 2 **40**, L334 (2000).
[3] M. Venkatesan, C. B. Fitzgerald, J. G. Lunney, and J. M. D. Coey, Phys. Rev. Lett. **93**, 177206 (2004).
[4] K. R. Kittilstved, N. S. Norberg, and D. R. Gamelin, Phys. Rev. Lett. **94**, 147209 (2005).
[5] J. H. Park, M. G. Kim, H. M. Jang, S. Ryu, and Y. M. Kim, Appl. Phys. Lett. **84**, 1338 (2004).
[6] Darshan C. Kundaliya, S. B. Ogale, S. E. Lofland, S. Dhar, C. J. Meeting, S. R. Shinde, Z. Ma, B. Varughese, K. V. Ramanujachary, L. Salamanca-Riba, and T. Venkatesan, Nat. Mater. **3**, 709 (2004).
[7] G. Lawes, A. S. Risbud, A. P. Ramirez, and R. Seshadri, Phys. Rev. B **71**, 045201 (2005).
[8] A. S. Risbud, N. A. Spaldin, Z. Q. Chen, S. Stemmer, and R. Seshadri, Phys. Rev. B **68**, 205202 (2003).
[9] C. J. Cong, L. Liao, J. C. Li, L. X. Fan, and K. L. Zhang, Nanotechnology **16**, 981 (2005); S. Deka, R. Pasricha, and P. A. Joy, Chem. Mater. **16**, 1168 (2004).
[10] J. Blasco, F. Bartolomé, L. M. García, and J. García, J. Mater. Chem. **16**, 2282 (2006); S. Thota T. Dutta, and J. Kumar, J. Phys.: Condens. Matter **18**, 2473 (2006).
[11] K. R. Kittilsved, W. K. Liu, and D. R. Gamelin, Nat. Mater. **5**, 291 (2006).
[12] Neeraj Khare, Menno J. Kappers, Ming Wei, Mark G. Blamire, and Judith L. MacManus-Driscoll, Adv. Mater. (Weinheim, Ger.) **18**, 1449 (2006).
[13] D. A. Schwartz and D. R. Gamelin, Adv. Mater. (Weinheim, Ger.) **16**, 2115 (2004).
[14] K. R. Kittilstved, D. A. Schwartz, A. C. Tuan, S. M. Heald, S. M. Chambers, and D. R. Gamelin, Phys. Rev. Lett. **97**, 037203 (2006).
[15] J. M. D. Coey, M. Venkatesan, and C. B. Fitzgerald, Nat. Mater. **4**, 173 (2005).
[16] A. Calleja, X. Casas, I. G. Serradilla, M. Segarra, A. Sin, P. Odier, and F. Espiell, Physica C **372**, 1115 (2002).
[17] B. L. Chamberland, A. W. Sleight and J. F. Weiher, J. Solid State Chem. **1**, 512 (1970). After the completion of this paper we became aware of a recent publication by J. Blasco and J. García, J. Solid State Chem. **179**, 2199 (2006), where it is stated that $ZnMnO_3$ is indeed a cubic spinel with SG *Fd*3*m* and a nominal stochiometry $Mn_{1+x}Zn_{2-x}O_4$ (x=0.3–0.4).
[18] D. Rubi, J. Fontcuberta, J. Arbiol, A. Calleja, Ll. Aragonés, X. G. Capdevila, and M. Segarra (unpublished).
[19] P. Sharma, A. Gupta, K. V. Rao, F. J. Owens, R. Sharma, R. Ahuja, J. M. Osorio Guillen, B. Johansson, and G. A. Gehring, Nat. Mater. **2**, 673 (2003).
[20] O. D. Jayakumar, I. K. Gopalakrishnan, C. Sudakar, R. M. Kadam, and S. K. Kulshreshta, cond-mat/0610170.
[21] A. C. Tuan, J. D. Bryan, A. B. Pakhomov, V. Shutthanandan, S. Thevuthasan, D. E. McCready, D. Gaspar, M. H. Engelhard, J. W. Rogers, K. Krishnan, D. R. Gamelin, and S. A. Chambers, Phys. Rev. B **70**, 054424 (2004).
[22] H. J. Kim, I. C. Song, J. H. Sim, H. Kim, D. Kim, Y. E. Ihm, and W. K. Choo, Phys. Status Solidi B **241**, 1553 (2004).
[23] S. Kolesnik, B. Dabrowski, and J. Mais, J. Supercond. **15**, 251 (2002).
[24] M. A. García, M. L. Ruiz-González, A. Quesada, J. L. Costa-Krämer, J. F. Fernández, S. J. Khatib, A. Wennberg, A. C. Ca-

ballero, M. S. Martín-González, M. Villegas, F. Briones, J. M. González-Calbet, and A. Hernando, Phys. Rev. Lett. **94**, 217206 (2005).

[25] D. Rubi, A. Calleja, J. Arbiol, X. G. Capdevila, M. Segarra, Ll. Aragonés, and J. Fontcuberta, cond-mat/0608014, J. Magn. Magn. Matter (to be published).

[26] See review by Ü. Özgür *et al.*, J. Appl. Phys. **98**, 041301 (2005), and references therein.

[27] F. K. Shan, G. X. Liu, W. J. Lee, G. H. Lee, I. S. Kim, and B. C. Shin, Appl. Phys. Lett. **86**, 221910 (2005).

[28] Yingling Yang, Hongwei Yan, Zhengping Fu, Beifang Yang, Linsheng Xia, Yuadong Xu, Jian Zuo, Fanqing Li, Solid State Commun. **138**, 521 (2006).

[29] Yanfa Yan, S. B. Zhang, and S. T. Pantelides, Phys. Rev. Lett. **86**, 5723 (2001).

[30] S. W. Jung, S.-J. An, G.-C. Yi, C. U. Jung, S.-I. Lee, and S. Cho, Appl. Phys. Lett. **80**, 4561 (2002).

[31] B. Martínez, F. Sandiumenge, Ll. Balcells, J. Arbiol, F. Sibieude, and C. Monty, Appl. Phys. Lett. **86**, 103113 (2005).

[32] A. C. S. Sabioni, M. J. F. Ramos, and W. B. Ferraz, Mater. Res. **6**, 173 (2003).

[33] W. Gopel and U. Lampe, Phys. Rev. B **22**, 6447 (1980); W. Gopel, Surf. Sci. **62**, 165 (1977).

[34] P. Crespo, R. Litrán, T. C. Rojas, M. Multigner, J. M. de la Fuente, J. C. Sánchez-López, M. A. García, A. Hernando, S. Penadés, and A. Fernández, Phys. Rev. Lett. **93**, 087204 (2004).

[35] M. A. García, J. M. Merino, E. Fernández Piñél, A. Quesada, J. De la Venta, M. L. Ruiz Gonzalez, G. Castro, P. Crespo, J. Llopis, J. M. Gonzales-Calbet, and A. Hernando (unpublished).